

Research Article

José Luis Roca, German Rodríguez-Bermúdez, and Manuel Fernández-Martínez*

Fractal-based techniques for physiological time series: An updated approach

<https://doi.org/10.1515/phys-2018-0093>

Received Apr 24, 2018; accepted Jun 26, 2018

Abstract: Along this paper, we shall update the state-of-the-art concerning the application of fractal-based techniques to test for fractal patterns in physiological time series. As such, the first half of the present work deals with some selected approaches to deal with the calculation of the self-similarity exponent of time series. They include broadly-used procedures as well as recent advances improving their accuracy and performance for a wide range of self-similar processes. The second part of this paper consists of a detailed review of high-quality studies carried out in the context of electroencephalogram signals. Both medical and non-medical applications have been deeply reviewed. This work is especially recommended to all those researchers especially interested in fractal pattern recognition for physiological time series.

Keywords: Hurst exponent, self-similar process, fractal pattern, physiological time series, electroencephalogram

PACS: 05.40.Fb, 05.40.Jc, 05.45.Df, 05.45.Tp

1 Introduction

The word fractal derives from the Latin term “frangere”, that means “to break”. These mathematical objects are usually characterized by means of some key features we enumerate next:

- (i) Self-similarity. The subsets of a fractal set are exactly (approximate or statistically) equal to the whole set.

- (ii) Iterative nature. Indeed, fractal patterns may be artificially generated via algorithms. Also, a wide range of fractals can be endowed with a fractal structure naturally.
- (iii) Level of irregularity. The roughness that such objects show can be identified at a whole range of scales.
- (iv) Fractal dimension. The topological dimension of an object considered to exhibit fractal patterns is strictly lower than its Hausdorff dimension.

From the properties above, it holds that the fractal dimension is a single value containing useful information regarding fractal patterns on sets or processes. In fact, the study based on the calculation of the fractal dimension of a set becomes crucial nowadays to detect self-similar structures and patterns for a wide range of contexts and situations including health sciences, economy, and mathematical modelling. Another indicator of fractality, especially useful to be calculated or estimated in empirical applications involving time series, is the so-called Hurst exponent. It is worth pointing out that both quantities are theoretically connected throughout some formulae. For instance, $H = 1 + d - \dim_B$, where d is the Euclidean (embedding) dimension of the space and \dim_B denotes the standard box dimension. However, if we change the dimension function, then strong connections between such quantities still hold. For instance, it holds that $\dim(\alpha) = \frac{1}{H}$, where $\dim(\alpha)$ denotes a fractal dimension for curves (not necessarily continuous) with respect to an induced fractal structure (c.f. [1, Theorem 1]). So both the fractal dimension and the self-similarity index are somehow equivalent to study fractal patterns in random processes. We would like also to highlight the usefulness of such fractal-based techniques to explore for fractal patterns on electroencephalogram (EEG) signals. Interestingly, the information that such indicators may provide to researchers can be combined with Machine Learning tools. The first part of this paper contains a rigorous description regarding some of the most useful techniques to calculate the (unifractal) self-similarity exponent of time series. Our aim here is to highlight some selected algorithms to deal with fractal pattern recognition for those researchers interested in applying such techniques in the context of physiological

***Corresponding Author: Manuel Fernández-Martínez:** University Centre of Defence at the Spanish Air Force Academy, MDE-UPCT, 30720 Santiago de la Ribera, Murcia, Spain; Email: fmm124@gmail.com

José Luis Roca: University Centre of Defence at the Spanish Air Force Academy, MDE-UPCT, 30720 Santiago de la Ribera, Murcia, Spain; Email: jluis.roca@tud.upct.es

German Rodríguez-Bermúdez: University Centre of Defence at the Spanish Air Force Academy, MDE-UPCT, 30720 Santiago de la Ribera, Murcia, Spain; Email: german.rodriguez@tud.upct.es

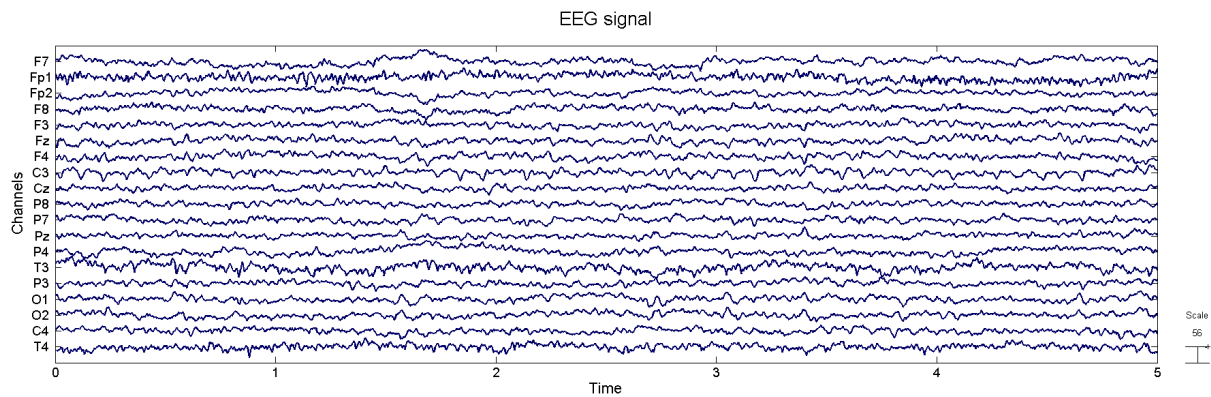


Figure 1: The picture above displays a 5 second EEG signal from a healthy subject sampled at 250 Hz by 19 channels

time series. For a description of fractal dimension based approaches, we refer the reader to [2], where other indicators for fractality including the correlation dimension as well as the Higuchi's and Katz's dimensions (to quote some of them) are described in detail.

Today, biosignals such as electrocardiogram, electromyogram, or EEG are acquired by many devices in real time [3]. That information can be analyzed throughout many techniques (both linear and nonlinear) that properly show the current state of the subject and even her/his evolution. This work is focused on EEG, which provides a representation of the electrical activity of the brain along the time [4]. Usually, that activity is collected using electrodes at several locations on the scalp via one electrode as a reference (placed in a different part) to measure the potential. The term channel is used to define the specific location of each electrode and the number of channels used changes depending on the pursued objective, being 2 to 128 the most usual numbers. The signal is sampled with frequencies ranging from 250 to 500 Hz and the amplitude usually varies about ± 100 μ V so it needs to be amplified. In general, researchers divide the EEG in different bands called delta (0.5 – 3 Hz), theta (4 – 7 Hz), alpha (8 – 13 Hz), beta (13 – 30 Hz), and gamma (> 30 Hz) [4]. Figure 1 depicts a 5-second EEG signal from a healthy subject, sampled at 250 Hz by 19 channels labeled according to the international 10/20 system.

Although the first motivation to acquire and study biosignals was mainly medical, the EEG signal analysis has increased widely along the last years due to the addition of non-medical and new applications including emotion recognition, neuromarketing, gaming, or Brain Computer Interfaces. It is worth mentioning that the present work is focused on fractal analysis as a way to study the brain dynamics.

The structure of this paper is as follows. In Section 2, we provide a rigorous description regarding some of the most representative fractal-based techniques to deal with the calculation of the self-similarity exponent of time series. In Section 3, some selected applications of this kind of approaches for EEG signal processing are collected. We would like to point out that top-quality contributions already published in JCR journals from year 2010 have been considered along this work. Thus, the main goal of the present work is to provide the reader and updated guide concerning the current state of applications of fractal-based techniques to such research fields.

2 Calculating the self-similarity exponent of random processes

In this section, we collect some selected procedures to appropriately calculate the self-similarity exponent of random processes. It is well-known that the Hurst exponent (more precisely, the self-similarity index or exponent) of a random process throws valuable information regarding trends and fractal patterns on data sets (in particular, time series). In other words, a great value of the self-similarity index indicator (*i.e.*, close to 1) means that some evidence regarding long-range dependence in the process under study may follow.

Some algorithms have been classically applied to estimate the self-similarity exponent of random processes. They include the classical R/S analysis and Detrended Fluctuation Analysis. However, other approaches appeared afterwards have been proved to be more versatile and accurate. Thus, Geometric method-based procedures and Fractal dimension algorithms constitute novel and ac-

curate alternatives especially useful to explore fractal patterns for short length series.

Anyway, the approaches described in the following subsections constitute a valuable selection to test for fractal patterns in physiological time series.

2.1 Mandelbrot's R/S analysis

The so-called R/S analysis is one of the most applied procedures to tackle with the estimation of the self-similarity exponent. It was first contributed by Mandelbrot and Wallis in [5] based on previous ideas due to English hydrologist H.E. Hurst (c.f. [6]). It is also worth mentioning that Mandelbrot first introduced the R/S analysis in economy (c.f. [7–9]) and argued that the performance of such a methodology is superior to variance, spectral, and autocorrelation analyses. The R/S analysis is especially appropriate to deal with large time series that could be modeled in terms of (fractional) Brownian motions.

For a time series (of returns) of length n and for each $m = 2^k < n$, divide it into $d = \frac{n}{m}$ non-overlapping blocks of length m . Then

1. For each block $\mathcal{B}_i = \{B_1, \dots, B_m\} : i = 1, \dots, d$, calculate both the mean, E_i , and the standard deviation, S_i .
2. Normalize the data of each block \mathcal{B}_i by subtracting its mean, E_i , i.e., let $N_j = B_j - E_i$, where $j = 1, \dots, m$.
3. Calculate the cumulative series (with mean 0) for each block \mathcal{B}_i : let $C_j = \sum_{k=1}^j N_k$ for $j = 1, \dots, m$.
4. Determine the range of C_j for each block, i.e., calculate $R_i = \max\{C_j : j = 1, \dots, m\} - \min\{C_j : j = 1, \dots, m\}$, where $i = 1, \dots, d$.
5. Rescale the range, i.e., calculate $\frac{R_i}{S_i}$ for $i = 1, \dots, d$.
6. Calculate the mean of the rescaled ranges, i.e., $RS_m = \frac{1}{d} \sum_{i=1}^d \frac{R_i}{S_i}$.
7. The self-similarity exponent of the time series calculated according to R/S Analysis, $H_{R/S}$, stands as the slope of the linear regression of $\log m$ vs. $\log RS_m$.

2.2 Detrended fluctuation analysis (DFA)

Detrended Fluctuation Analysis (DFA, hereafter), first contributed by Peng et al. (c.f. [10]), constitutes another broadly used approach to calculate the self-similarity index of random processes. It is noteworthy that it allows checking for correlation and scaling properties in time series (c.f. [11–13]). Thus, it becomes appropriate to study the evolution of the Hurst exponent of series which exhibit trends.

For a time series (of returns) of length n and for each $m = 2^k < n$, let us divide it into $d = \frac{n}{m}$ non-overlapping blocks of length m . Then

1. Determine the local trend of each block \mathcal{B}_i .
2. Let $Y_j : j = 1, \dots, m$ be the detrended process in each block \mathcal{B}_i , i.e., the difference between the original value of the series in the block and the local trend.
3. For each block, calculate $D_i = \frac{1}{m} \sum_{j=1}^m Y_j^2$ for $i = 1, \dots, d$.
4. Determine the statistic $F_m^2 = \frac{1}{d} \sum_{i=1}^d D_i$, namely, the mean variance of the detrended process.
5. The Hurst exponent calculated by DFA, H_{DFA} , stands as the slope of the linear regression of $\log m$ vs. $\log F_m$.

It is worth mentioning that both estimators, $H_{R/S}$ and H_{DFA} , throw information regarding memory in the series though not about the distribution of the increments of the corresponding process. Moreover, their definitions are both based on the variance (respectively, the standard deviation) of the process (respectively, its increments). However, even if such moments are infinite, such estimators still work properly (c.f. [14]). This fact implies, in particular, that when these estimators are applied to calculate the self-similarity exponent of either a Brownian motion or a Lévy stable motion with different self-similarity and without memory, then one gets $H_{R/S} = H_{DFA} = 0.5$.

2.3 Geometric method-based procedures (GM algorithms)

Geometric method-based procedures (GM algorithms, hereafter), GM1 and GM2, are both based on the next expression to estimate the self-similar exponent H of a random process:

$$\overline{\Delta B} \propto T_S^H,$$

where $\overline{\Delta B} = \overline{B(t + T_S) - B(t)}$ is the mean of the variation of B , the (log –)value of the series, on time intervals with lengths equal to T_S (c.f. [15, Section 4]). These approaches were first contributed by Sánchez-Granero et al. in [15] and revisited afterwards in terms of fractal structures (c.f. [16]). Next, we sketch their description in mathematical terms.

2.3.1 GM1

For a time series (of log-returns) of length n and for each $m = 2^k < n$, divide it into $d = \frac{n}{m}$ non-overlapping blocks of length m . Then

1. Calculate the variation of each block $\mathcal{B}_i = \{B_1, \dots, B_m\}$, i.e., let $D_i = B_m - B_1$ for $i = 1, \dots, d$.
2. Calculate the mean of the variations of all the blocks: $M_m = \frac{1}{d} \sum_{i=1}^d D_i$.
3. The self-similarity exponent of the time series calculated according to GM1 stands as the slope of the linear regression of $\log m$ vs. $\log M_m$.

2.3.2 GM2

Moreover, if additional information regarding the time series is available, e.g., if both the maximum and the minimum values of each period are known, then the following alternative to GM1 approach named GM2 may display valuable information concerning self-similar patterns and trends on the series.

For a time series (of log-returns) of length n and for each $m = 2^k < n$, divide it into $d = \frac{n}{m}$ non-overlapping blocks of length m . Then

1. Calculate the range of each block $\mathcal{B}_i = \{B_1, \dots, B_m\}$, i.e., let $R_i = \max\{B_j : j = 1, \dots, m\} - \min\{B_j : j = 1, \dots, m\}$ for $i = 1, \dots, d$.
2. Calculate the mean of the ranges of all the blocks: $M_m = \frac{1}{d} \sum_{i=1}^d R_i$.
3. The Hurst exponent of the time series calculated by GM2 is the slope of the linear regression of $\log m$ vs. $\log M_m$.

It is worth mentioning that both GM1 and GM2 approaches consider the log-values of the series, whereas R/S analysis uses the (log) returns. Interestingly, the validity of these geometrical procedures to properly calculate the self-similarity exponent of (fractional) Brownian motions and (fractional) Lévy stable motions has already been justified theoretically (c.f. [16, Corollaries 3.5 and 3.9]). Additionally, in that work, the authors described both GM algorithms in terms of fractal structures (c.f. [16, Section 3]). Thus, they constitute two accurate geometrical methods to test for scaling and correlation properties on time series.

2.4 FD algorithms

Fractal dimension algorithms (FD algorithms, hereafter), were introduced from the viewpoint of fractal structures by

Sánchez-Granero et al. in [1], where their accuracy to calculate the self-similarity exponent of a broad range of random processes was theoretically proved. Moreover, it was verified by Monte Carlo simulation that the three FD algorithms, FD1, FD2, and FD3 work properly for short series. Next, we describe how to calculate the self-similarity index of random processes throughout FD algorithms. With this aim, we shall utilize the concept of a fractal structure.

Firstly, recall that a family Γ of subsets of X is a covering of X if $X = \cup\{A : A \in \Gamma\}$. Thus, a fractal structure on a set X is defined as a countable family of coverings of X , $\Gamma = \{\Gamma_n : n \in \mathbb{N}\}$, such that the two following conditions stand for all natural numbers:

- (i) For each $A \in \Gamma_{n+1}$, there exists $B \in \Gamma_n$ such that $A \subseteq B$.
- (ii) Each $B \in \Gamma_n$ can be written as $B = \cup\{A \in \Gamma_{n+1} : A \subseteq B\}$.

In other words, the covering Γ_{n+1} is a strong refinement of Γ_n , called level n of Γ . If $\alpha : [0, 1] \rightarrow \mathbb{R}$ is a parameterization of a real curve and $\Gamma = \{\Gamma_n : n \in \mathbb{N}\}$ is the fractal structure on $[0, 1]$ with levels given by $\Gamma_n = \left\{ \left[\frac{k}{2^n}, \frac{k+1}{2^n} \right] : k = 0, 1, \dots, 2^n - 1 \right\}$, then we can define a fractal structure on the image set of α , $\alpha(I)$, by $\Delta = \{\Delta_n : n \in \mathbb{N}\}$ where $\Delta_n = \{\alpha(A) : A \in \Gamma_n\}$ (c.f. [1, Definition 1]). Further, let l denote the length of the time series, hereafter.

– FD1:

1. Let d_n be the mean of $\{\text{diam}(A) : A \in \Delta_n\}$ for $1 \leq n \leq \log_2 l$, where $\text{diam}(A) = \sup\{|x - y| : x, y \in A\}$.
2. Define $r_n = \frac{d_{n+1}}{d_n}$ for $1 \leq n \leq \log_2 l - 1$.
3. Calculate r as the mean of $\{r_n : 1 \leq n \leq \log_2 l - 1\}$.
4. The self-similarity exponent of the series calculated according to FD1 is given by $H = -\log_2 r$.

It is worth noting that FD1 is valid to calculate the parameter of random processes satisfying the condition $E[X_n] = 2^H \cdot E[X_{n+1}]$. In particular, it works properly if $X_n \sim 2^H \cdot X_{n+1}$, which is the case of processes with stationary and self-affine increments with parameter H (c.f. [1, Theorem 1]). In addition, it holds that GM2 is also valid to calculate the parameter of random processes lying under the condition

$$E[X_1] = 2^{(n-1)H} \cdot E[X_n].$$

Since such an equality is equivalent to $E[X_n] = 2^H \cdot E[X_{n+1}]$, then the validity of GM2 approach is equivalent to the validity of FD1 for Hurst exponent calculation purposes.

- FD2: Given a random variable X , recall that its s -moment is defined by $m_s(X) = E[X^s]$ for $s > 0$, provided that such an expected value exists. Let $X_k = M(2^{-k}, \omega)$ for each $k \in \mathbb{N}$, where $M(T, \omega) = M(0, T, \omega)$ and

$$M(t, T, \omega) = \sup_{t \leq s \leq t+T} \{Y(s, t, \omega)\} - \inf_{t \leq s \leq t+T} \{Y(s, t, \omega)\},$$

where $Y(s, t, \omega) = X(s, \omega) - X(t, \omega)$. It is worth pointing out that $\{\text{diam}(A) : A \in \Delta_k\}$ is a sample of the random variable $M(2^{-k}, \omega)$ (c.f. [1, Remark 1]). Hence, the FD2 approach can be described in the following terms.

1. Calculate $y_s = \{y_{k,s} : 1 \leq k \leq \log_2 l - 1\}$, where $y_{k,s} = \frac{m_s(X_k)}{m_s(X_{k+1})}$.
2. Let \bar{y}_s be the mean of each list y_s .
3. Calculate the point s_0 such that $\bar{y}_{s_0} = 2$. Notice that $\{(s, \bar{y}_s) : s > 0\}$ is s -increasing.
4. The self-similarity exponent calculated via FD2 is given by $H = \frac{1}{s_0}$ (c.f. [1, Theorem 1]).

It turns out that FD2 approach is valid to appropriately calculate the parameter of random processes lying under the condition

$$E \left[X_n^{\frac{1}{H}} \right] = 2 \cdot E \left[X_{n+1}^{\frac{1}{H}} \right]$$

(c.f. hypothesis (2) in [1, Theorem 3]). In particular, it holds for random functions such that

$$X_n^{\frac{1}{H}} \sim 2 \cdot X_{n+1}^{\frac{1}{H}}.$$

Going beyond, if $X_n \sim 2^H \cdot X_{n+1}$, then $X_n^{\frac{1}{H}} \sim 2 \cdot X_{n+1}^{\frac{1}{H}}$, and hence, both [1, Theorem 1] and [1, Theorem 3] guarantee that FD2 is valid to estimate the parameter of processes with self-affine and stationary increments with parameter H .

- FD3: Next, we describe the so-called FD3 algorithm, an alternative to FD2 approach, which is also based on [1, Theorem 3].

1. Calculate $\{(k, \beta_{k,s}) : 1 \leq k \leq \log_2 l\}$, where $\beta_{k,s} = \log_2 m_s(X_k)$. Let β_s be the slope of the regression line of $\{(k, \beta_{k,s}) : 1 \leq k \leq \log_2 l\}$.
2. Calculate s_1 such that $\beta_{s_1} = -1$.
3. The Hurst exponent calculated through FD3 is given by $H = \frac{1}{s_1}$ (c.f. [1, Theorem 1]).

Thus, FD3 procedure is valid to calculate the parameter of random processes satisfying the identity

$$E \left[X_n^{\frac{1}{H}} \right] = \frac{1}{2^{n-1}} \cdot E \left[X_1^{\frac{1}{H}} \right].$$

Since such an expression is equivalent to

$$E \left[X_n^{\frac{1}{H}} \right] = 2 \cdot E \left[X_{n+1}^{\frac{1}{H}} \right],$$

then FD3 is valid to calculate the self-similarity exponent of a random process with stationary and self-affine increments with parameter H , if and only if, FD2 is.

3 Applications of fractal analysis to analyse physiological time series

Fractal-based techniques have been widely applied for physiological time series to extract valuable information and analyze dynamical properties underlying subjects' biosignals. Despite a wide range of biophysiological signals may be acquired and saved by diverse electronic devices, in this paper we shall be focused on some highlighted applications regarding EEG signals.

Usually, biosignal acquisition has been related to unhealthy subjects. However, along the last years healthy subjects are increasingly using biosignals in several applications. Next, we comment on some of them in the field of EEG.

Electroencephalogram signals (EEGs, hereafter) are potential fluctuations recorded from the scalp due to the brain electrical activity. It is worth pointing out that EEGs may be collected in distinct cognitive states or environments [17] and mathematically modeled as time series. The information extracted via fractal analysis becomes useful in medical and non-medical applications [18]. In the present paper, we have been focused on papers already appeared in *Journal Citation Reports'* publications from 2010.

3.1 Medical applications

It is assumed that EEGs do reflect the brain dynamics, and hence, pathological states. This is the reason for which fractal and multifractal analyses have been extensively applied to medical biosignals in the last years [19]. The main clinical applications are surveyed next.

3.1.1 Epilepsy

Epilepsy is a neurological disorder leading patients to suffer spontaneous seizures. In each seizure, brain produces unexpected electrical discharges in a oscillatory state [20]. It is a common neurological disorder suffered by nearly 1% of the world population [21, 22]. An early detection of epilepsy becomes crucial to improve patients' quality of life. It is worth pointing out that epilepsy diagnosis has

been carried out via a visual inspection of EEGs by experts. In this way, different approaches to deal with epileptic seizure prediction from EEGs have been provided by scientists without requiring human inspection [23].

Since EEGs are identified as nonlinear systems and epileptic seizures are sudden excessive electrical discharges in a group of neurons, it is reasonable that nonlinear techniques may become appropriate for seizure identification and detection [24].

With the aim to develop an automated system to detect epileptic seizures, fractal analysis has been applied for feature extraction as descriptors of the structure of EEGs which have been classified later by several machine learning based algorithms. In 2011, Yuan [24] characterized EEGs by extracting features via DFA and approximate entropy and classified them via an extreme learning machine. A satisfying recognition accuracy of 96.5% was reported. In 2012, Quang *et al.* [22] combined the ICA (Independent Component Analysis) with the Largest Lyapunov Exponent to clean EEGs. Further, Acharya *et al.* [25] combined both Hurst exponent and fractal dimension with other features achieving high accuracy from a small number of features. In 2013, Zhou conducted wavelet decomposition on EEGs with five scales and selected the wavelet coefficients [26]. Effective features including lacunarity and fluctuation index were extracted from the selected scales and then sent to a Bayesian Linear Discriminant obtaining satisfactory results. In 2015, Fergus *et al.* [23] extracted some features via the correlation dimension and mixed them with frequency domain features. They were ranked and then a classifying based on a k -nearest neighbor was conducted. Their results improved the performance of previous studies by as much as 10% in most cases. Nazami *et al.* [27] contributed a study regarding EEGs using both the Hurst exponent and the fractal dimension. The results of such analyses reported that they are able to forecast the onset of a seizure on an average of 25.76 seconds before the time of occurrence. In 2016, Upadhyay *et al.* [28] presented a comparative study among distinct feature ranking techniques for epileptic seizure detection. In this occasion, the EEGs were decomposed by means of 16 discrete wavelets. Several wavelet-based techniques for feature extraction including Katz's, Petrosian, and Higuchi's dimensions were involved in such a study where Higuchi's and Katz's threw the best results.

3.1.2 Depth of anesthesia

The anesthesia monitoring becomes crucial to guarantee a safety and comfortable scenario to work along a medi-

cal intervention [29]. Despite novel monitoring approaches have been applied to characterize EEGs [30–32], there is not an overall agreement regarding the automated depth of anesthesia monitoring: it constitutes an old problem in the literature and also a key aspect to tackle with. In fact, a high level of anesthesia may lead to over dosing effects. Nevertheless, a low level of substance may lead patients to suffer intra-operative awareness [29]. With this aim, a wide range of techniques for time series analysis including correlation dimension and Largest Lyapunov Exponents have been applied. However, they have not achieved a total acceptance due to their limitations to entirely describe the properties of the EEGs [33, 34]. The main limitation of fractal-based methods lies in the fact that EEGs usually display non-uniform and complex fluctuations leading to distinct fractal dimension values for a given brain state. Thus, fractal dimension methods may not describe accurately such signals [34]. Despite that, the performance of novel proposals for anesthesia monitoring are compared with fractal based techniques [35]. For instance, in 2017, Khulman and Manton [36] proposed auto-regressive moving average as a measure for anesthesia monitoring and compared it with Higuchi's fractal dimension obtaining similar results. Interestingly, the medical equipment industry have developed the so-called Bispectral Index Score, currently the reference measure [29], though the incidence of awareness still remains for further research.

3.1.3 Autism

Autism Spectrum Disorder (ASD) constitutes a group of complex neurodevelopmental disorders, characterized by deficits in social communication and interaction, and restricted, repetitive, and stereotyped patterns of behavior. Individuals diagnosed with ASD have co-occurring intellectual disability, language disorder, and epilepsy at higher rates than the general population [37].

It holds that EEG analysis becomes a powerful tool to detect ASD. In 2010, Ahmadlou *et al.* [38] presented a paper entitled "Fractality and a Wavelet-Chaos-Neural Network" for ASD diagnosis where they were compared Higuchi's and Katz's methods for fractal dimension computation. The best results were achieved by Katz's dimension.

3.1.4 Depression

Depression is a common and serious psychiatric disorder. It is generally characterized by feelings such as sadness, fatigue, discouragement, helplessness, despair, or hope-

lessness that continue for several months or longer [39]. The analysis of EEGs may reveal information concerning the evolution of the brain signal affected by depression [40, 41]. Despite the high incidence in the population, diagnosis for depression mainly consists on a combination of both an interview and a questionnaire about the observation of subjective symptoms.

Higuchi's and Katz's dimensions combined with wavelet-chaos techniques were used as indicators of depressive disorders by Ahmadlou *et al.* [42]. Authors claimed that Higuchi's dimension shows meaningful differences between both healthy and depressive groups. In 2013, band power, Higuchi's dimension, DFA, correlation dimension, and Largest Lyapunov Exponents were considered as classifiers to discriminate depression patients and normal controls [40]. The same year, Bachmann *et al.* [41] computed spectral asymmetry index and Higuchi's dimension as features, obtaining similar results for depression identification. Later, in 2015, Acharya *et al.* [43] presented the novel Depression Diagnosis Index with satisfactory results. That work, fractal dimension, Largest Lyapunov Exponents, sample entropy, DFA, higher order spectra, and recurrence quantification analysis were involved for feature extraction and then combined.

3.1.5 Parkinson, Alzheimer, and schizophrenia

Alzheimer's disease is a type of dementia characterized by the gradual destruction of the patient's brain cells, neurofibrillary tangles, and senile plaques in different widespread brain regions [44]. In 2011, Ahmadlou *et al.* [45] applied both Katz's and Higuchi's dimensions as markers of abnormality in Alzheimer's disease. Later, in 2016, Smith *et al.* [46] reported that Higuchi's dimension becomes sensitive to brain activity changes typical in healthy aging and Alzheimer's disease.

Other application consists of characterizing Parkinson's disease (PD, hereafter). The pathophysiology of PD is known to involve altered patterns of neuronal firing and synchronization in cortical-basal ganglia circuits. One window into the nature of the aberrant temporal dynamics in the cerebral cortex of PD patients can be derived from analysis of the patients electroencephalography [47]. Only a few published works characterize PD via fractal analysis of time series. In 2016 appeared an interesting study where emotions in Parkinson subjects were detected by means of approximate entropy, correlation dimension, DFA, fractal dimension, higher order spectrum, Largest Lyapunov Exponents, and sample entropy for feature extraction [48].

On the other hand, schizophrenia is a severe and persistent debilitating psychiatric disorder that affects approximately 0.4–0.6% of the world's population. Patients show disturbances in thoughts, affects, and perceptions, as well as difficulties in relationships with others [49]. In 2011, Sabeti *et al.* [49] applied fractal dimension combined with power spectrum and autoregressive coefficients to distinguish schizophrenic patients and control participants reporting satisfactory results. In 2016, Yu *et al.* [50] computed the box-counting dimension to estimate the cool executive function of EEG data recorded from first-episode schizophrenia patients and healthy controls during the performance of three cool executive function tasks. Results showed that the fractal dimension was different in first-episode schizophrenia patients during the manipulation of an executive function.

3.2 Non-medical applications

As it was stated above, fractal-based techniques have been also applied to deal with non-medical biosignals. Below we review some of them.

3.2.1 Brain Computer Interface

A Brain Computer Interface (BCI) system acquires and analyzes EEG signals to allow a direct communication and control pathway from the human brain to a computer [51]. At the beginning, BCI was used as a medical tool to allow communication or movements of people with severe disabilities. However, in the last years, researchers have applied BCI systems in different areas such as gaming, home automation, communication systems, robotics, . . . , etc [52].

Although linear features have been intensively used in BCI systems [52, 53], nonlinear techniques have been also applied to tackle with BCI applications. In 2010, Hsu [54] applied wavelet fractal features in a motor imagery paradigm BCI system to identify the movement of both the left and right hands. The next year, multiresolution fractal feature vectors were computed as well as a modified fractal dimension from wavelet data to develop an asynchronous BCI system [55]. Later, in 2013, it was presented an study based on multiresolution fractal feature vectors for Motor Imagery BCI [56]. On the other hand, in 2011, Esfahani *et al.* [57] used Largest Lyapunov Exponents with band power features to identify the satisfaction of the user in human-robot interaction. Also, Katz's and Higuchi's dimensions, R/S analysis, and Renyi's entropy

were tested by Loo *et al.* [58] to carry out a detailed comparison involving some feature extraction techniques in motor imagery-based BCI. It is worth pointing out that the best results were achieved by Katz's dimension together with a fuzzy k -nearest neighbors classifier. In 2013, Wang and Sourina [59] presented a novel method to recognize mental arithmetic tasks for multifractal analysis of EEG signals named generalized Higuchi's fractal dimension spectrum. Additionally, they were extracted power spectrum, autoregressive coefficients, and statistical features from EEGs. The results achieved got improved in both multi-channel and one-channel subject-dependent algorithms. Later, in 2015, Rodríguez *et al.* developed a study involving three approaches (DFA, GM2, and Generalized Hurst Exponent) for self-similarity exponent calculation purposes and compared them to deal with feature extraction in Motor Imagery Based Brain Computer Interface Systems [60].

3.2.2 Emotion recognition

It is worth mentioning that a real-time approach based on EEG emotion recognition may lead researchers to new pathways in human computer interaction involving many applications including entertainment, education, and medical applications to name a few [61].

A technology for biosignal analysis could be more interesting than some already existing emotion recognition systems based on the user's face or gestures since it could allow to reflect the "true" emotion of the user [62].

In 2012, Sourina *et al.* [62] proposed an emotion recognition algorithm allowing to recognize 6 different emotions in real-time. The emotions were generated by using the International Affective Digitized Sounds (IADS). That work, fractal dimension values were computed by both box-counting and Higuchi's algorithms and them used for feature classification.

4 Conclusions

This article provides an updated state-of-the-art regarding some applications of fractal-based techniques to test for fractality patterns in physiological time series. Firstly, we technically describe several approaches to properly deal with the calculation of the self-similarity exponent of a time series. They include broadly-used algorithms as well as recent procedures improving their accuracy and performance for a wide range of self-similar processes. In addition, we contribute a detailed review involving some

high-quality studies developed in the context of electroencephalogram signals. Both medical and non-medical applications are deeply reviewed and commented as well.

Acknowledgement: The last author is partially supported by grants No. MTM2015-64373-P from Spanish Ministry of Economy and Competitiveness and No. 19219/PI/14 from Fundación Séneca of Región de Murcia.

References

- [1] Sánchez-Granero M.A., Fernández-Martínez M., Trinidad Segovia J.E., Introducing fractal dimension algorithms to calculate the Hurst exponent of financial time series, *Eur. Phys. J. B*, 2012, 85: 86, <https://doi.org/10.1140/epjb/e2012-20803-2>
- [2] Rodríguez-Bermúdez G., García-Laencina P.J., Analysis of EEG Signals using Nonlinear Dynamics and Chaos: A review, *Appl. Math. Inf. Sci.*, 2015, 9, 2309-2321.
- [3] Palaniappan R., *Biological Signal Analysis*, Ventus Publishing ApS, 2010.
- [4] Schomer D. L., Da Silva F. L., *Niedermeyer's Electroencephalography, Basic Principles, Clinical Applications, and Related Fields*, 6th ed., Lippincott Williams & Wilkins, 2011.
- [5] Mandelbrot B.B., Wallis J.R., Robustness of the rescaled range R/S in the measurement of noncyclic long run statistical dependence, *Water Resour. Res.*, 1969, 5, 967-988.
- [6] Hurst H.E., Long-term storage capacity of reservoirs, *Transactions of the American Society of Civil Engineers*, 1951, 116, 770-799.
- [7] Mandelbrot B.B., When Can Price be Arbitraged Efficiently? A Limit to the Validity of the Random Walk and Martingale Models, *Rev. Econ. Stat.*, 1971, 53, 225-236.
- [8] Mandelbrot B.B., Statistical Methodology for Nonperiodic Cycles: From the Covariance to R/S Analysis, *Annals of Economic and Social Measurement*, 1972, 1, 259-290.
- [9] Mandelbrot B.B., *Fractals and Scaling in Finance. Discontinuity, Concentration, Risk*. Selecta Volume E, 1st ed., Springer-Verlag, New York, 1997.
- [10] Peng C.-K., Buldyrev S.V., Havlin S., Simons M., Stanley H.E., Goldberger A.L., Mosaic organization of DNA nucleotides, *Phys. Rev. E*, 1994, 49, 1685-1689.
- [11] Ausloos M., Statistical physics in foreign exchange currency and stock markets, *Physica A*, 2000, 285, 48-65.
- [12] Di Matteo T., Aste T., Dacorogna M.M., Long-term memories of developed and emerging markets: Using the scaling analysis to characterize their stage of development, *J. Bank Financ.*, 2005, 29, 827-851.
- [13] Liu Y., Cizeau P., Meyer M., Peng C.-K., Stanley H.E., Correlations in economic time series, *Physica A*, 1997, 245, 437-440.
- [14] Montanari A., Taqqu M.S., Teverovsky V., Estimating long-range dependence in the presence of periodicity: An empirical study, *Math. Comput. Model.*, 1999, 29, 217-228.
- [15] Sánchez Granero M.A., Trinidad Segovia J.E., García Pérez J., Some comments on Hurst exponent and the long memory processes on capital markets, *Physica A*, 2008, 387, 5543-5551.

- [16] Trinidad Segovia J.E., Fernández-Martínez M., Sánchez-Granero M.A., A note on geometric method-based procedures to calculate the Hurst exponent, *Physica A*, 2012, 391, 2209-2214.
- [17] Stam C.J., Nonlinear dynamical analysis of EEG and MEG: Review of an emerging field, *Clin. Neurophysiol.*, 2005, 116, 2266-2301.
- [18] Wang Q., Sourina O., Nguyen M.K., Fractal dimension based neurofeedback in serious games, *Visual Comput.*, 2011, 27, 299-309.
- [19] Lopes R., Betrouni N., Fractal and multifractal analysis: A review, *Med. Image Anal.*, 2009, 13, 634-649.
- [20] Iasemidis L.D., Sackellares J.C., The evolution with time of the spatial distribution of the largest Lyapunov exponent on the human epileptic cortex, In: Duke, D.W. and Pritchard, W.S. (Eds.), *Measuring Chaos in the human brain*, World Scientific, Singapore, 1991.
- [21] Mormann F., Andrzejak R.G., Elger C.E., Lehnertz K., Seizure prediction: the long and winding road, *Brain*, 2007, 130, 314-333.
- [22] Dang Khoa T.Q., Minh Huong N.T., Van Toi, V., Detecting Epileptic Seizure from Scalp EEG Using Lyapunov Spectrum, *Comput. Math. Method Med.*, 2012, <http://dx.doi.org/10.1155/2012/847686>
- [23] Fergus P., Hignett D., Hussain A., Al-Jumeily D., Abdel-Aziz K., Automatic Epileptic Seizure Detection Using Scalp EEG and Advanced Artificial Intelligence Techniques, *Biomed Res. Int.*, 2015, <http://dx.doi.org/10.1155/2015/986736>
- [24] Yuan Q., Zhou W., Li S., Cai D., Epileptic EEG classification based on extreme learning machine and nonlinear features, *Epilepsy Res.*, 2011, 96, 29-38.
- [25] Acharya U.R., Sree S.V., Chuan Alvin A.P., Yanti R., Suri J.S., Application of non-linear and wavelet based features for the automated identification of epileptic EEG signals, *Int. J. Neural Syst.*, 2012, 22, <https://doi.org/10.1142/S0129065712500025>
- [26] Zhou W., Liu Y., Yuan Q., Li X., Epileptic Seizure Detection Using Lacunarity and Bayesian Linear Discriminant Analysis in Intracranial EEG, *IEEE Trans. Biomed. Eng.*, 2013, 60, 3375-3381.
- [27] Namazi H., Kulish V.V., Hussaini J., Hussaini J., Delaviz A., Delaviz F., Habibi S., Ramezani S., A signal processing based analysis and prediction of seizure onset in patients with epilepsy, *Oncotarget*, 2016, 7, 342-350.
- [28] Upadhyay R., Padhy P.K., Kankar P.K., A comparative study of feature ranking techniques for epileptic seizure detection using wavelet transform, *Comput. Electr. Eng.*, 2016, 53, 163-176.
- [29] Cusenza M., Fractal analysis of the EEG and clinical applications, PhD thesis, Università degli studi di Trieste, Italy, 2012.
- [30] Shoushtarian M., Sahinovic M.M., Absalom A.R., Kalmar A.F., Vereecke H.E.M., Liley D.T.J., Struys M.R.F., Comparisons of Electroencephalographically Derived Measures of Hypnosis and Antinociception in Response to Standardized Stimuli During Target-Controlled Propofol-Remifentanyl Anesthesia, *Anesth. Analg.*, 2016, 122, 382-392.
- [31] Shalbaf R., Behnam H., Moghadam H.J., Monitoring depth of anesthesia using combination of EEG measure and hemodynamic variables, *Cogn. Neurodynamics*, 2015, 9, 41-51.
- [32] Shalbaf R., Behnam H., Sleight J.W., Steyn-Ross A., Voss L.J., Monitoring the depth of anesthesia using entropy features and an artificial neural network, *J. Neurosci. Methods*, 2013, 218, 17-24.
- [33] Pradhan C., Jena S.K., Nadar S.R., Pradhan N., Higher-Order Spectrum in Understanding Nonlinearity in EEG Rhythms, *Comput. Math. Method Med.*, 2012, <http://dx.doi.org/10.1155/2012/206857>
- [34] Zoughi T., Boostani R., Deypir M., A wavelet-based estimating depth of anesthesia, *Eng. Appl. Artif. Intell.*, 2012, 25, 1710-1722.
- [35] Kuhlmann L., Freestone D.R., Manton J.H., Heyse B., Vereecke H.E.M., Lipping T., Struys M.M.R.F., Liley D.T.J., Neural mass model-based tracking of anesthetic brain states, *NeuroImage*, 2016, 133, 438-456.
- [36] Kuhlmann L., Manton J.H., Heyse B., Vereecke H.E.M., Lipping T., Struys M.M.R.F., Liley D.T.J., Tracking Electroencephalographic Changes Using Distributions of Linear Models: Application to Propofol-Based Depth of Anesthesia Monitoring, *IEEE Trans. Biomed. Eng.*, 2017, 64, 870-881.
- [37] Buckley A.W., Scott R., Tyler A., Matthew Mahoney J., Thurm A., Farmer C., Swedo S., Burroughs S.A., Holmes G.L., State-Dependent Differences in Functional Connectivity in Young Children With Autism Spectrum Disorder, *EBioMedicine*, 2015, 2, 1905-1915.
- [38] Ahmadlou M., Adeli H., Adeli A., Fractality and a Wavelet-Chaos-Neural Network Methodology for EEG-Based Diagnosis of Autistic Spectrum Disorder, *J. Clin. Neurophysiol.*, 2010, 27, 328-333.
- [39] Akar S.A., Kara S., Agambayev S., Bilgiç V., Nonlinear analysis of EEG in major depression with fractal dimensions, In: *Engineering in Medicine and Biology Society (EMBC), 37th Annual International Conference of the IEEE*, 2015, 7410-7413.
- [40] Hosseini Fard B., Hassan Moradi M., Rostami R., Classifying depression patients and normal subjects using machine learning techniques and nonlinear features from EEG signal, *Comput. Meth. Programs Biomed.*, 2013, 109, 339-345.
- [41] Bachmann M., Lass J., Suhhova A., Hinrikus H., Spectral Asymmetry and Higuchi's Fractal Dimension Measures of Depression Electroencephalogram, *Comput. Math. Method Med.*, 2013, <http://dx.doi.org/10.1155/2013/251638>
- [42] Ahmadlou M., Adeli H., Adeli A., Fractality analysis of frontal brain in major depressive disorder, *Int. J. Psychophysiol.*, 2012, 85, 206-211.
- [43] Acharya U.R., Sudarshan V.K., Adeli H., Santhosh J., Koh J.E.W., Puthankatti S.D., Adeli A., A Novel Depression Diagnosis Index Using Nonlinear Features in EEG Signals, *Eur. Neurol.*, 2015, 74, 79-83.
- [44] Mizuno T., Takahashi T., Cho R.Y., Kikuchi M., Murata T., Takahashi K., Wada Y., Assessment of EEG dynamical complexity in Alzheimer's disease using multiscale entropy, *Clin. Neurophysiol.*, 2010, 121, 1438-1446.
- [45] Ahmadlou M., Adeli H., Adeli A., Fractality and a Wavelet-chaos-Methodology for EEG-based Diagnosis of Alzheimer Disease, *Alzheimer Dis. Assoc. Dis.*, 2011, 25, 85-92.
- [46] Smits F.M., Porcaro C., Cottone C., Cancelli A., Rossini P.M., Tocchio F., Electroencephalographic Fractal Dimension in Healthy Ageing and Alzheimer's Disease, *PLoS One*, 2016, <https://doi.org/10.1371/journal.pone.0149587>
- [47] Lainscsek C., Hernandez M.E., Weyhenmeyer J., Sejnowski T.J., Poizner H., Non-linear dynamical analysis of EEG time series distinguishes patients with Parkinson's disease from healthy individuals, *Front. Neurol.*, 2013, <https://doi.org/10.3389/fneur.2013.00200>
- [48] Yuvaraj R., Murugappan M., Hemispheric asymmetry non-linear analysis of EEG during emotional responses from idiopathic Parkinson's disease patients, *Cogn. Neurodynamics*, 2016, 10, 225-234.

- [49] Sabeti M., Katebi S.D., Boostani R., Price G.W., A new approach for EEG signal classification of schizophrenic and control participants, *Expert Syst. Appl.*, 2011, 38, 2063-2071.
- [50] Yu Y., Zhao Y., Si Y., Ren Q., Ren W., Jing C., Zhang H., Estimation of the cool executive function using frontal electroencephalogram signals in first-episode schizophrenia patients, *Biomed. Eng. Online*, 2016, 15: 131, <https://doi.org/10.1186/s12938-016-0282-y>
- [51] Wolpaw J.R., Birbaumer N., McFarland D.J., Pfurtscheller G., Vaughan T.M., Brain-computer interfaces for communication and control, *Clin. Neurophysiol.*, 2002, 113, 767-791.
- [52] Nicolas-Alonso L.F., Gomez-Gil J., Brain Computer Interfaces, a Review, *Sensors*, 2012, 12, 1211-1279.
- [53] Lotte F., Congedo M., Lécuyer A., Lamarche F., Arnaldi B., A review of classification algorithms for EEG-based brain-computer interfaces, *J. Neural Eng.*, 2007, 4, R1-R13.
- [54] Hsu W.-Y., EEG-based motor imagery classification using neuro-fuzzy prediction and wavelet fractal features, *J. Neurosci. Methods*, 2010, 189, 295-302.
- [55] Hsu W.-Y., Continuous EEG signal analysis for asynchronous BCI application, *Int. J. Neural Syst.*, 2011, 21, 335-450.
- [56] Hsu W.-Y., Single-trial motor imagery classification using asymmetry ratio, phase relation, wavelet-based fractal, and their selected combination, *Int. J. Neural Syst.*, 2013, 23, <https://doi.org/10.1142/S012906571350007X>
- [57] Esfahani E.T., Sundararajan V., Using brain-computer interfaces to detect human satisfaction in human-robot interaction, *Int. J. Humanoid Robot.*, 2011, 8, 87-101.
- [58] Loo C.K., Samraj A., Lee G.C., Evaluation of Methods for Estimating Fractal Dimension in Motor Imagery-Based Brain Computer Interface, *Discrete Dyn. Nat. Soc.*, 2011, <http://dx.doi.org/10.1155/2011/724697>
- [59] Wang Q., Sourina O., Real-Time Mental Arithmetic Task Recognition From EEG Signals, *IEEE Trans. Neural Syst. Rehabil. Eng.*, 2013, 21, 225-232.
- [60] Rodríguez-Bermúdez G., Sánchez-Granero M.A., García-Laencina P.J., Fernández-Martínez M., Serna J., Roca-Dorda J., Testing the Self-Similarity Exponent to Feature Extraction in Motor Imagery Based Brain Computer Interface Systems, *Int. J. Bifurcation Chaos*, 2015, 25, <https://doi.org/10.1142/S0218127415400234>
- [61] Calvo R.A., D'Mello S., Affect Detection: An Interdisciplinary Review of Models, Methods, and Their Applications, *IEEE Trans. Affect. Comput.*, 2010, 1, 18-37.
- [62] Sourina O., Liu Y., Nguyen M.K., Real-time EEG-based emotion recognition for music therapy, *J. Multimodal User Interfaces*, 2012, 5, 27-35.